Growth of Fe on MgO(001) studied by He-atom scattering

G. Fahsold* and A. Pucci
Universität Heidelberg, Kirchhoff-Institut für Physik, Albert-Ueberle-Strasse 3-5, 69120 Heidelberg, Germany

K.-H. Rieder
Freie Universität Berlin, Institut für Experimentalphysik, Arnimallee 14, 14195 Berlin, Germany
(Received 19 February 1999)

With He-atom scattering we studied the epitaxial growth of Fe ultrathin films deposited on *in situ* cleaved MgO(001). The measurements at various substrate temperatures ($140 \leqslant T \leqslant 670$ K) start with bare MgO(001) and extend to film thicknesses beyond the complete coverage of the substrate. From the development of specular intensity with Fe deposition we estimate saturation island densities, give a quantitative description of the evolution of their size and shape, and calculate a thickness for coalescence of all islands. The observed three-dimensional metal island growth behavior is suppressed at low temperature (140 K) where a monolayer film almost completely covers the substrate. For increased substrate temperatures a decreased island density and an increased interlayer mass transport from substrate level onto the islands leads to a temperature and thickness dependent change in island shape.

I. INTRODUCTION

There is growing interest in the preparation and the surface properties of ultrathin metal films on metal oxide surfaces. Depending on the application field and the electronic properties of interest either the controlled formation of metal islands or the preparation of homogenous thin films is emphasized. Metal island films on MgO are widely tested for designed catalytic properties. On the other hand the search for magnetic properties of homogenous Fe films on MgO,[1] which is due to the interest in magnetic recording media, has been stimulated by the predicted high magnetic moment of the monolayer.[2] Until now, uncertainties in the film morphological properties have inhibited the experimental verification of this prediction. Therefore, the basic aspects of metal-on-oxide growth are still of current interest.

Due to its catalytic applications and its chemical, thermal, and mechanical stability, MgO has widely been used as a substrate for metallic thin films.[1,3–5] Ultraclean single crystalline MgO(001) is easily prepared by cleavage in ultrahigh vacuum (UHV). Several attempts to prepare clean surfaces from air-cleaved crystals have been done,[1,6] but both contaminants (from air or segregations as a result of high temperature treatment) and structural (or stoichiometric) defects reduce the quality of these surfaces.[7] It is well known that the quality of the substrate and of its surface are of great relevance for the morphology of deposited metal films.[3,8,9] The evidently different surface quality of MgO samples cleaved in UHV and in air leads to different metal film growth modes, as shown by a comparative He-atom scattering (HAS)-reflection and IR-transmission study.[10]

Due to the low lattice mismatch between bcc-Fe(001) and MgO(001) (lattice spacings at room temperature are 4.06 Å for Fe along ⟨110⟩ and 4.20 Å for MgO along ⟨100⟩) MgO is a very good substrate candidate for an epitaxial growth of Fe on an insulator.[1,6,8] From LEED observations[6] and *ab initio* calculations[2] the Fe atoms are supposed to sit above the oxygen atoms. There has been some discrepancy in the literature concerning the growth mode of Fe on MgO(001). A layer-by-layer growth from the beginning of deposition[6] is in contradiction with magnetic properties, static and dynamic conductivity measurements.[1,11–13] The higher surface free energy of Fe [2.9 J/m^2 (Ref. 14)] compared to MgO(001) [1.1 J/m^2 (Ref. 15)] favors three-dimensional island formation. For an understanding of mechanic, catalytic, and electromagnetic properties of Fe/MgO(001), detailed information on, e.g., the density of growing islands and the development of their shape is needed.

He-atom scattering is a favorable nondestructive method for ionic crystal surface investigations. Photons, electrons, or high-energy ions may deteriorate the surface quality and influence the growth behavior of adsorbates. Due to its high surface sensitivity He-atom diffraction yields structural information on the outermost atomic layer. Metal island distributions and island shapes may be investigated.[16] There are no restrictions concerning electrical properties of the sample surface, which is the main advantage over charged particle scattering methods or scanning tunneling microscopy (STM).

This paper reports on elastic HAS studies of the growth of Fe on MgO(001) for substrate temperatures from 140 to 670 K. After a short description of the theoretical background (Sec. II) and the experimental setup (Sec. III) the results from our HAS experiments are described (Sec. IV). We discuss these results (Sec. V) with respect to details of the observed subsequent phases of thin-film growth. The conclusions (Sec. VI) point at a method to prepare smooth layered films of this metal-insulator system.

II. THEORETICAL BACKGROUND

Deviations of the distribution of scattered intensity from the ideal diffraction patterns are related to the disorder of the sample, i.e., in atom scattering, to the lateral density, the dimensions, and the orientation of surface defects such as, e.g., steps, facets, and isolated or clustered adatoms.[17,18] The attenuation of specularly reflected intensity with the growth

of adatom islands could be described easily if the islands contribute only negligibly to the total diffraction intensity. This is well fulfilled for most molecular or rare gas adsorbates due to their thermal disorder.[18] For the system under investigation, the Debye temperature of the metal adsorbate is smaller only by a factor of about 2 than that of the ionic crystal substrate. Hence, adlayer contributions to specular reflectivity should be taken into account unless they are suppressed, e.g., by short-range roughness or by facetting. Since both the structural properties characterize the iron islands on MgO(001), i.e., the first one at lower temperature, the second one at higher values, we neglect diffractional contributions from adsorbates and islands. Then, the specularly reflected intensity $I(d)$ decays with increasing average film thickness d as

$$\frac{I(d)}{I_0} = 1 - \sigma_i(d) n_i(d) - \sigma_a n_a(d), \tag{1}$$

where I_0 is the intensity reflected from the bare substrate surface, $\sigma_i(d)$ is the average cross section of the growing islands, and $n_i(d)$ is the number of islands per unit area. σ_a and $n_a(d)$ stand for the cross section and the amount of mobile adsorbates which are present on the substrate surface during deposition. Equation (1) describes the two contributions to the attenuatuion $1 - I/I_0$ as stains produced by adsorbates or islands from adsorbates on the otherwise perfect surface mirror.[18]

As the area of uncovered substrate surface decreases with increasing number of deposited particles, the amount of mobile adsorbates per unit area should depend on the average film thickness d. Concerning the cross sections defined by Eq. (1) it is well known that for very low coverage σ_i and σ_a seen by He atoms are strongly enhanced compared to the geometric cross sections. This enhancement is typically quantified by a surrounding scattering halo of ~ 10 Å width.[4,18,19] σ_i of the smallest stable clusters and σ_a reach values $\geqslant 10^2$ Å^2. For high coverage, the overlap of single island cross sections leads to a reduction of the total cross section. In this case, the reflected intensity may still be described by the linear dependence on the total cross section as done in Eq. (1), but the single-island cross section has to be substituted by the geometric cross section.[18] The density of scattering adsorbate islands $n_i(d)$ increases with film thickness d according to the nucleation rate, which depends on the substrate surface and the substrate temperature. Nevertheless, for attractive high-mobility adatom systems, as most metal-on-ionic-crystal systems are, a saturation density n_s is often reached at a still low substrate coverage.[4,20]

III. EXPERIMENT

Our He-atom scattering experiments were performed with an apparatus consisting of an UHV chamber, a thermal-energy He-atom source and a single-atom He detector. Following the He-atom beam, the source part consists of a temperature stabilized closed-cycle cooled nozzle, a skimmer, and two apertures. The detector part is composed of a set of differentially pumped apertures and a quadrupole mass spectrometer (Balzers). This setup follows the basic concepts for He-atom diffraction and is described in detail by König.[21] For sample preparation the UHV chamber is equipped with a sample cleaver (VSW), a metal vapor source (Omicron EFM3), and a three-axis manipulator (Thermionics) holding a molybdenum plate with the mounted sample. A resistive heater and a liquid nitrogen heat exchanger allow access to sample temperatures between 140 and 1000 K. The temperature at the sample plate is measured with a type K thermocouple. The metal-vapor flux from an Fe rod (2 mm diameter, purity $>99.9\%$) heated by electron bombardment is aligned perpendicularly to the sample surface to avoid shadowing by substrate surface steps. This flux was calibrated by observing He-atom diffraction intensity oscillations during layer-by-layer growth at Fe(001) homoepitaxy. Deposition rates of typically 1 Å /min were chosen. Film thicknesses are given in units of an epitaxial monolayer (ML) with a thickness of $h_{\mathrm{ML}} = 1.33$ Å, i.e., 1.13×10^{15} metal atoms/cm^2 on MgO(001).

We used cylinder shaped MgO crystals[22] with a (001) base plane of 10 mm diameter and an initial length of about 10 mm. These crystals were mounted on the molybdenum sample plate described above. At room temperature and under UHV conditions (residual gas pressure $<2 \times 10^{-10}$ mbar) slabs of about 2 mm thickness were cleaved off along a $\langle 100 \rangle$ direction leading to substrate surfaces of reproducible quality as verified by HAS reflectivities.[23] We observed a weak deterioration of these surfaces in UHV with time (typically days), but after heating the crystals to 670 K the original reflectivities could be reestablished within 5%. The remaining differences in the quality of our substrate surfaces are probably the main origin of the scatter in our data.

For our HAS experiments, a beam energy of typically 20 meV with a velocity spread $\delta v/v \simeq 0.02$ was used. At this energy perpendicular momentum transfer leads to in-phase specular scattering from terrace levels both on the substrate and on the Fe surface with a high sensitivity for adsorbates.[18] Additionally, for scattering of the bare substrate surface along $\langle 100 \rangle$, the first order diffracted beams are well separated from the specular beam but they still lie within the accessible angular range. Under this condition, peak profiles and background structure are best resolved.

The scattering angle is fixed at 90° and the sample surface is rotated around an axis perpendicular to the scattering plane. Crystal alignment is done by maximizing specular and first-order peak intensities, keeping the two first-order peak intensities at a balance. A step motor drive allowed to reproduce the angle of incidence (measured with respect to the surface normal) within 0.009°. With this set-up we recorded specular-intensity curves during Fe thin-film growth with a sampling time of typically one hundred data points per growing ML. For recording angular diffraction data we interrupted the metal deposition for typically 5 min. As we will demonstrate, these interruptions do not remarkably influence the growth of thin films for substrate temperatures between 140 and 670 K.

IV. RESULTS

The results of our HAS specular intensity measurements are shown in Fig. 1 for the various substrate temperatures. Prior to metal deposition the surfaces of UHV-cleaved MgO(001) show high intensities which are typically

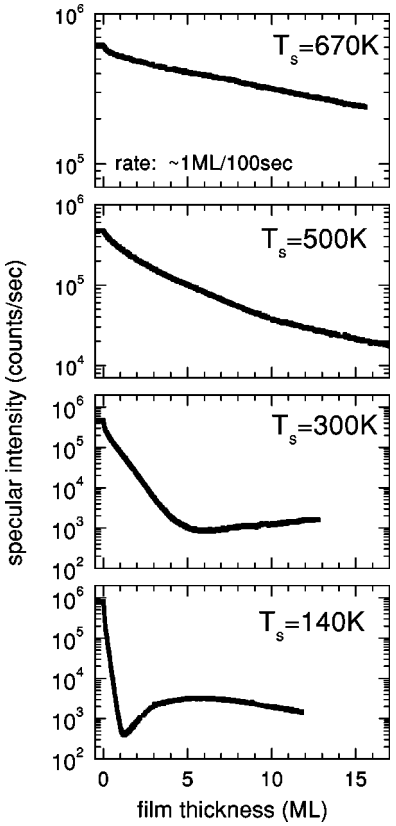

FIG. 1. Intensity of specularly-scattered He atoms during deposition of Fe on MgO(001) at various substrate temperature T_s, as indicated.

6×10^5 counts/sec for our experimental setup. The differences in these finite absolute intensities cannot be reasonably explained by a Debye-Waller factor since the data belong to different samples. In the very beginning of metal deposition we find a fast decay of specular intensity (see, e.g., Fig. 2 which focuses on the early growth stages). The thickness range for this initial decay period decreases with decreasing temperatures from ~1 ML at 670 K to ~0.1 ML at 140 K (~0.4 ML in Fig. 2). The subsequent intensity behavior is well described by an exponential decay that is easily verified by the logarithmic plots in the figures. With further increasing film thickness the specular reflectivity deviates from that behavior. For 500 K the intensity quickly starts to approach a constant value of about 10^4 counts/sec for a film thickness above ~10 ML. In contrast to this, for 300 K the intensity reaches a broad intensity minimum of ~900 counts/sec at 6 ML, and at 140 K a sharp minimum of ~400 counts/sec is reached already at 1.2 ML. At 140 K an increase of specular intensity follows approaching ~3000 counts/sec at ~5 ML. Then the intensity slowly decays again.

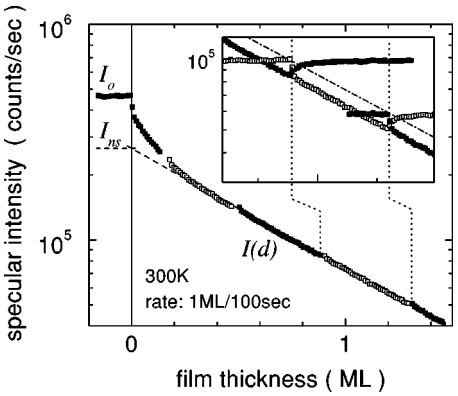

FIG. 2. Development of specular intensity $I(d)$ during deposition of Fe on MgO(001) at 300 K. The start of deposition (initial period) and subsequent deposition periods are indicated by alternately full and open symbols. The initial intensity I_0 and the extrapolated zero-thickness intensity I_{ns} are indicated. The inset additionally shows the development of reflectivity upon opening and closing the shutter of the evaporator. The dash-dotted line shows the intensity corrected for mobile adsorbates, i.e., $(1+f)I(d)$ (see Sec. IV).

Figure 2 shows the development of specular intensity on opening and closing the evaporator shutter. The intensity curves for subsequent deposition periods at 300 K are pasted in this figure to demonstrate the influence of interruptions of the deposition on the measured reflected intensity and on overall growth behavior. Such interruptions of the growth were necessary for taking angular scans of intensity. On opening and closing the evaporator shutter (see inset of Fig. 2) the reflectivity decreases and increases again. This behavior is due to a population of mobile adsorbates on the substrate surface (see Sec. II). We analyzed this mobile adsorbate induced reduction of reflected intensity in more detail and we found that the reduction is governed by diffusion on MgO(001), that it drops with temperature increase, and that it is proportional (with factor f) to the reflected intensity, hence

$$\sigma_a n_a(d) = f\frac{I(d)}{I_0}. \tag{2}$$

With Eq. (1), for the total island cross section follows:

$$\sigma_i(d) n_i(d) = 1-(1+f)\frac{I(d)}{I_0}. \tag{3}$$

We determined f to be $\leqslant 0.2$ for the substrate temperatures in Fig. 1. Concerning the overall growth behavior, the pasted intensity curves well indicate that the interruptions of the deposition do not result in severe distortions of the growth behavior. The intensity curves of subsequent growth periods appear with the same slope.

The angular distributions of scattered intensity shown in Fig. 3 help to get more insight into the film morphologies. Sharp specular and first-order diffraction peaks at 25°, 45°, and 65° supply evidence for the quality of the long range (>200 Å) periodic corrugation of the substrate surface. For all substrate temperatures of investigation the intensities of the first-order diffraction peaks decay simultaneously with the decreasing specular intensity. However, while at highest temperature (670 K) the peak shapes and the diffraction background remain essentially unchanged, new scattering features are developed at temperatures below 670 K. At 500 K and for a thickness >10 ML, e.g., we find a strong and broadly footed specular intensity contribution [with a FWHM of ~4% of the Brillouin zone (BZ)] which is absent for the first order diffraction peaks. At 140 K well distinguished specular peak shoulders (separation ~10% of BZ) already arise at ~0.2 ML. For further deposition, during the

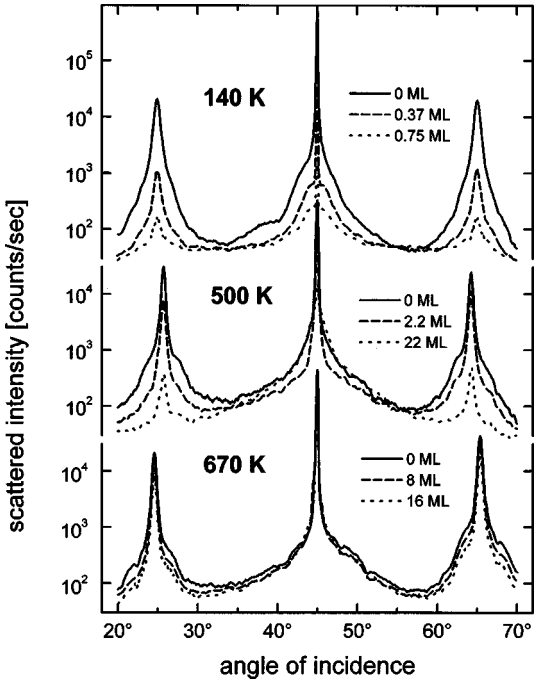

FIG. 3. Angular distribution of intensity scattered from ultrathin Fe island films on MgO(001) grown at three different substrate temperatures (as labeled). The various film thicknesses are given in the figure and are indicated by different line types.

intensity reincrease (for temperatures $\leqslant 300$ K) these shoulders turn into a broader specular diffraction peak (FWHM $\sim 10\%$ of BZ) which is accompanied by first-order diffraction peaks of increasing intensity.

Additionally, we also performed ex-situ atomic force microscopy (AFM) measurements of MgO(001) and in-situ low-energy electron diffraction (LEED) measurements of both the substrate and the films grown at various temperatures. The AFM pictures of MgO(001) display terraces, typically a few 100 Å wide and several microns long, with terrace edges preferentially along [100] and [010]. We found $p(1\times1)$ LEED patterns for the surfaces of the substrate cleaved in UHV and of the Fe films grown at various temperatures and fully covering these substrates. On closer inspection, a film of 110 Å thickness grown at 400 K exhibited a fourfold splitting of the diffraction peaks (see Fig. 4).

V. DISCUSSION

For all substrate temperatures under investigation there are qualitative similarities in the experimental results for the development of specular reflectivity with Fe coverage (see Fig. 1) which allow a distinction between different phases of thin-film growth. Following the increase of film thickness, we term these phases nucleation (for the initial fast decay), island growth (for the following moderate decay), complete substrate coverage (at the minimum of reflectivity), island smoothing (the following increase of intensity), and homoepitaxial growth (for the final decay of specular intensity). In the following subsections, after a short discussion of these growth phases, we will analyze our data with respect to island densities, island shapes, and island sizes, complete substrate coverage, and their dependence on substrate temperature.

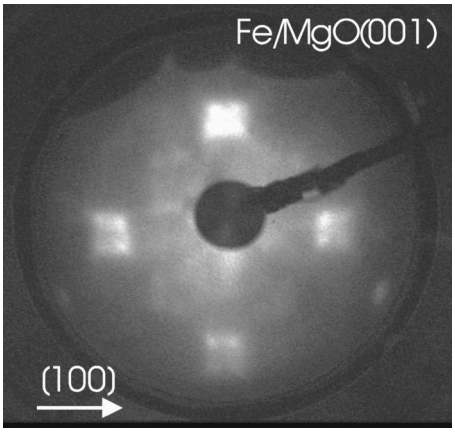

FIG. 4. LEED pattern from 110 Å thick Fe/MgO(001) grown at 400 K. Horizontal is along [100] of MgO(001), the energy is 193.5 eV .

A. Phases of thin-film growth

Nucleation and growth of islands. At the beginning of metal deposition the specular intensity, decreasing at first rapidly and then moderately, indicates the nucleation and the growth of islands. For the following reasons, this intensity (which will be used in Secs. V B and V C for the quantitative description of the island structure) is dominated by the scattering of the uncovered substrate surface. First, the ratio of diffraction peak intensities and the shapes of these peaks remain almost unchanged over a specular intensity decay of more than one order of magnitude (see first order peaks, e.g., in Fig. 3). Both shape and relative intensity of a peak are defined by the corrugation of the crystalline surface potential, by the terrace width distribution, and by the phonon structure.[18,24] For example, due to the smaller surface potential corrugation of metals compared to ionic crystals,[24,25] a stronger decay of higher order diffraction intensity is expected if metal surface scattering contributes to the peaks. Secondly, we have a chemical argument for dominantly substrate surface scattering. It is based on our observation that exposure to oxygen affects the scattering from the MgO(001) substrate by less than 1%, whereas for a completely Fe covered annealed surface the intensity decreases by more than a factor of 10. For 2 ML Fe grown at room temperature we find the specular intensity has decreased by only a factor of ~ 0.8 after exposure to 1 L oxygen at room temperature.

Complete substrate coverage. Substrate surface scattering is observed until the minimum of reflectivity is reached (see curves for 140 and 300 K in Fig. 1). In the thickness range around the minimum of specular reflection the surface appears with maximum roughness. For low substrate temperatures (140 K) where the minimum of reflectivity is equal to the background scattering rate, this maximum roughness is reached at a thickness just prior to coalescence of all the islands, i.e., the substrate surface is fully covered by such diffusely scattering islands. With further deposition smoothing of the surface starts. For deposition at 300 K we find the HAS intensity minimum with a value that is only two times higher than the reflectivity minimum for 140 K. Therefore, we interpret it also as an indication of complete substrate coverage. From our recent IR-spectroscopical investigations follows that the similarly prepared films become continuous

at a film thickness that agrees with this HAS minimum.[12] Around the thickness of this minimum (5.7 ML or 8 Å) and for the same system and growth temperature, Liu *et al.*[13] observe a gradual transition of the temperature dependence of the dc conductivity from abnormal (disordered 2D) to normal (3D) behavior. Nevertheless, the large surface roughness and the residual holes in the metal film may complicate or perturb LEED observations, magnetic measurements[13] and STM imaging[11] (see Sec. V D).

Island smoothing. After complete coverage is achieved, at 300 K and below, the significant increase of reflectivity (see Fig. 1) indicates the transition of surface morphology. The growth changes from heteroepitaxial to homoepitaxial and the long-range roughness, which is the result of the preceding island growth, transforms to a homoepitaxial roughness. The reasons for this transient growth are the changes of diffusion barriers and of surface free energy minimization arguments as soon as complete substrate coverage is achieved. The observation that at a constant deposition rate ($\sim 10^{-2}$ ML/sec) the smoothing of the surface is faster at 140 K than at room temperature seems to be in contradiction with the respective adatom mobilities. Actually, growth at room temperature develops larger islands (see Secs. V B and V C), which need more mass to be wiped out again.

Homoepitaxial growth. On prolonged metal deposition homoepitaxial growth kinetics should induce further changes of surface morphology. For example, at 140 K the finally decreasing reflectivity indicates that roughness is increasing again, well known, e.g., from Fe homoepitaxy.[26] Growth at temperatures above 300 K creates flat regions at the surface. We observed high scattering intensities for homoepitaxial growth of Fe on very thick films at 500 K (Ref. 23) but also the development of facets at 400 K (see fourfold LEED spots in Fig. 4). Homoepitaxial facetting is known for Fe between 400 and 450 K (Ref. 27) due to Ehrlich-Schwoebel-barriers.[28] For growth at, e.g., 500 K and at high coverage (see Fig. 1) the specular reflectivity decay deviates from an exponential behavior, so that due to specular scattering from the metal facets Eq. (3) is no longer valid (see detailed discussion below). Strong shoulders of the specular peak indicate the respective contribution (see Fig. 3, curves for 2.2 and 22 ML grown at 500 K).

B. Density of growing islands

From the transition in the intensity curves from an initial decay to an exponential behavior we estimate the saturation island density n_s which is reached, e.g., after deposition of about 0.4 ML at 300 K (see Fig. 2). The density n_s will be gained by application of Eq. (3) to the island-growth phase [where $n_i(d)$ has reached the saturation value n_s and $I(d)$ shows an exponential behavior]. Independence from island size is achieved by extrapolating $I(d)$ and $\sigma(d)$ to zero film thickness. This leads to I_{ns} (see Fig. 2) and to the nonvanishing cross section σ_0. Then, Eq. (3) gives

$$n_s = \left(1-(1+f)\frac{I_{ns}}{I_0}\right)\sigma_0^{-1}. \tag{4}$$

The island cross section σ_0 of a just nucleated island should approximately be ~ 500 Å^2, as it was determined for the mean cross section for vanishing metal island size from a combined HAS-TEM study of Pd/MgO(001).[4] In the case of overestimation of the true cross section, e.g., due to an overlap of cross sections, Eq. (4) will underestimate the true saturation island densities.[18]

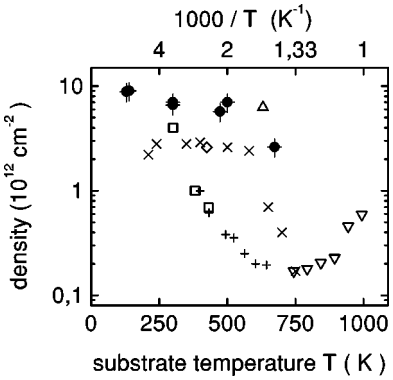

FIG. 5. Saturated island density n_s for Fe/MgO(001) (●, our data), island density of 1 ML Fe on MgO(001) cleaved in air (△, Ref. 29), island densities for 10 nm thick Fe films on polished MgO(001) (∇, Ref. 30), and grain densities of continuous thin films of Fe/MgO(001) (□, Ref. 11, and ◇, from thinnest film in Ref. 27). For comparison, saturated island densities for Pd on MgO(001) (+, Ref. 4, and ×, Ref. 31).

With Eq. (4) and $\sigma_0 = 500$ Å^2, we calculated n_s for our data. The dependence of n_s on the substrate temperature is shown in Fig. 5. The high value at lowest temperature (8×10^{-2} ML at 140 K) corresponds to a mean island distance of ~ 33 Å. As this distance is just above the diameter of the stable cluster cross section σ_0, we believe that the true island density is only slightly underestimated by our HAS data analysis. This is corroborated by other experimental findings. At 140 K, e.g., we observe a nucleation period according to about ~ 0.03 ML (at a rate of 1 ML per 100 sec). If we assume that during this nucleation period all atoms impinging on the substrate form stable dimers, we get an island density of about 2×10^{13} cm^{-2}, which is only little above the calculated n_s value.

With an x-ray scattering method, for Fe/MgO(001) grown at 630 K Lairson *et al.*[29] find an island spacing which well corresponds with our results for n_s (see Fig. 5). We also compare our results with cluster densities (calculated from mean grain sizes) of Fe continuous films on MgO(001) measured by STM (Refs. 11,27) (see Fig. 5). As local conductivity is needed for taking STM data, these films on MgO already cover the substrate completely. However, their granular morphologies give at least lower limit estimates of n_s of the preceding island growth. While at ~ 300 K the cluster densities evaluated from the continuous films are close to our HAS findings for the island films, the cluster densities are far below our results at temperatures >300 K. Probably, coagulation of islands[29] or of grains in the continuous films[27] is the main reason for this difference in the results. Very recent AFM measurements[30] for 10 nm thick Fe/MgO(001) deposited at various very high temperatures (from 700 to 1000 K) find island densities which for the highest temperature should correspond to seperate islands on MgO(001). This density value shows a high compatibility with the global trend of our results (see Fig. 5).

Although our densities underestimate the true saturation

island density, they are already far above typical values found in the past for island films of other metals (e.g., Pd, Au, Ag, Cu) on various ionic substrates (MgO, NaCl, KBr). In Fig. 5 they are represented by data for Pd/MgO(001) from Ref. 4. In contrast, a very recent AFM study[31] of the same system shows island densities and a temperature dependence (see Fig. 5) which both are much closer to our results for n_s.

Several reasons could be responsible for the high values and the low temperature dependence of Fe island densities on MgO(001). Compared to noble metals and Pd, e.g., the transition metal Fe shows a higher cohesive energy, a large electronegativity difference of 1.9 with respect to oxygen, and, compared to alkali halides, MgO has a high dielectric constant, i.e., the image potential of an adsorbate is stronger. These facts favor stable cluster formation and reduce the mobility of both adatoms and clusters. In addition, traplike defects increase the island density and, as calculated for Pd/MgO(001),[31] suppress within certain limits its diffusion related temperature dependence. A temperature dependence reappears with reducing the adatom mobility. In the case of Fe/MgO(001), the monomer diffusion barrier should be no smaller than 0.4 eV [which is calculated for Cu/MgO(001) (Ref. 32)]. Compared to 0.2 eV for Pd/MgO(001),[31] this higher barrier might be the reason for the weak temperature dependence between 140 and 500 K, which should not be confused with post-nucleation or post-growth phenomena as known from many microscopy studies.[20]

There is strong evidence for an increased defect density on air-cleaved MgO(001).[3,10,33] For UHV-cleaved MgO the nature of trapping defects with a concentration $\geqslant 10^{12}\,\mathrm{cm}^{-2}$ is not clarified. While we find regular steps at distances (along $\langle 110\rangle$) of $\sim$120 Å for all our UHV-cleaved MgO(001) samples,[23] the high trapping energy of 1.5 eV observed for Pd/MgO(001) seems to support point defects.[31] Irrespective of the nature of the defects, the resulting high saturation island densities support a rapid substrate coverage (see Sec. V D).

C. Evolution of size and shape of growing islands

In the thickness range of island growth where the specular reflected intensity $I(d)$ decays exponentially with coverage d (in units of the epitaxial monolayer thickness $h_{\mathrm{ML}}=1.33$ Å), a temperature-dependent lateral growth parameter γ can be considered:

$$\gamma = -\frac{\partial}{\partial d}\ln I(d). \tag{5}$$

The experimental results for γ are values around unity at room temperature which decay by about two orders of ten with increasing temperature (see Fig. 6). In the following we will explain how γ as a growth parameter describes the development of island size with increasing film thickness.

The intensity specularly reflected from a surface which is covered by a fixed number (saturation density n_s) of growing islands is approximated by

$$\frac{I(d)}{I_{ns}} = 1 - a(d)n_s. \tag{6}$$

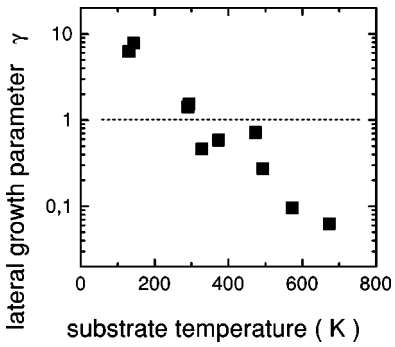

FIG. 6. Lateral growth parameter γ (see text) determined from exponential decay of reflectivity during island growth of Fe/MgO(001) at various temperatures.

In this formulation of Eq. (1), we used $\sigma(d)\simeq a(d)$ (a is the average geometric cross section of an island without halo) to account for the high substrate coverage according to the large n_s values.[18] For the exponential intensity decay from Eq. (5), Eq. (6) relates $a(d)$ to the saturation value $1/n_s$ according to

$$a(d) = (1 - e^{-\gamma d})n_s^{-1}. \tag{7}$$

This growth behavior is different from a power law as applied recently by Henry and Meunier to the growth kinetics of small coverages of metal clusters on oxide surfaces.[34] Here we have to consider high coverages of the surface due to the high values for n_s (see Fig. 5) and a growth up to almost complete coverage.

The exponential growth of island size can be understood by looking at the increase of island area which is proportional to the uncovered substrate surface area:

$$\frac{\partial a}{\partial d} = \gamma[n_s^{-1} - a(d)]. \tag{8}$$

If γ equals unity all atoms impinging on the bare substrate surface contribute to the increase of island area, i.e., there is no desorption and no mass transport from the substrate-surface level onto the islands. If there is such mass transport, γ should be smaller than unity. On the other hand, a mass transport from a higher level down to the substrate level, which, e.g., is necessary for layer-by-layer growth, should be indicated by γ larger than one. In each case, Eq. (8) describes a multilayer-growth mode, as there is metal-vapor flux on both the still uncovered and the already covered fraction of substrate surface area.

A diffusion of adatoms into the substrate or a desorption of adatoms might influence the interpretation of γ. For the system under investigation we neglect both these possibilities. Instead, we assume complete condensation since an estimation of the desorption rate gives a value of about eight orders of magnitude smaller than the deposition rate. Additionally, the chemical and mechanical stability of MgO does not seem to allow appreciable metal diffusion into the substrate.

The reason for the temperature dependence of γ (see Fig. 6) should be the fact that island border lines may act as diffusion barriers. In the case of Fe homoepitaxy[27] so-called Ehrlich-Schwoebel barriers[28] hamper the spreading of ada-

toms and thus cause the formation of facets. At room temperature, where we find $\gamma \simeq 1$, adatoms from the substrate surface are hindered from increasing the height of a metal island by jumping onto this island. Instead, adatoms presumably are trapped at the island border, which increases the lateral dimension of the island. The larger number of neighboring metal atoms on top of an existing island should energetically favor the more three-dimensional configuration of a Fe cluster, but the effort to break the adsorbate-substrate bond inhibits the minimization of surface-free energy. Accordingly, the islands grow in a multilayer mode out of thermal equilibrium.

At temperatures above room temperature the smaller values for γ indicate a mass transport from the substrate onto Fe islands, i.e., Fe adatoms more easily overcome the substrate-island diffusion barrier. With increasing substrate temperature the growth of islands approaches strong 3D growth which corresponds to thermal equilibrium of metals on perfect ionic crystal surfaces.

At temperatures below 300 K, the experimental values for γ suggest a mass transport down from the metal islands, which really means a tendency towards 2D growth. However, it has to be considered that these Fe islands do not exceed atomic dimensions. As the adatom mobility is nearly frozen at 140 K the growth regime is more statistical.[20] In terms of our model, the very small cluster size is responsible for the increased lateral growth. A similar growth phenomenon is known, e.g., from Pt homoepitaxy, leading to a reentrant layer-by-layer growth.[35]

We now turn to the consequences of the observed growth behavior on the development of island shape. According to Eq. (7) the area $a(d)$ of a metal island exponentially approaches the complete-coverage value n_s^{-1}. The single island volume v has to increase proportional to the amount of deposited metal, i.e.,

$$v(d) = d h_{\mathrm{ML}} n_s^{-1} \tag{9}$$

(changes of mass density are not considered). Since $v(d)/a(d)$ and $a(d)^{1/2}$ are different functions of d, the height-to-diameter ratio (aspect ratio), i.e., the island shape, changes during growth. A dependence of island shape on both growth temperature and film thickness is often ignored in literature.

Above room temperature, due to the small lateral growth rates and the small island densities, the islands grow with a large aspect ratio compared to the lower temperatures. To contain the total deposited mass this ratio should be of the order of unity for an island. As {011} surfaces show the smallest free surface energy for Fe, we assume (001) and {011} planes as possible island facets. This corresponds to the LEED results of Fig. 4. Consequently the islands should form truncated or stepped regular pyramids.

At 670 K, due to the high adatom mobility, these pyramidlike islands presumably grow layer-by-layer-like starting from the island boarder line in a step flow growth mode. We expect the (001) facet to be of minor weight, which is due to the largest height-to-diameter ratio (compared to the lower temperatures) and due to the absence of HAS diffraction structure in our angular scans along $\langle 110 \rangle$. At 500 K, the lateral growth increases faster than the island density, this means a reduction of aspect ratio. The (001) facets, which are larger with respect to 670 K, offer smooth surface area for HAS reflection as observed in the reflectivity and in the angular scans. With further reduction of temperature the islands should spread laterally and the fraction of (001) area should further increase. But the concurrent reduction of adatom mobility hinders the development of regular shapes and smooth surfaces, which is indicated by the small reflectivities at room temperature and below. At 140 K, the fast coverage of the surface does not allow conclusions on island shape in the low coverage regime within the above mentioned approach.

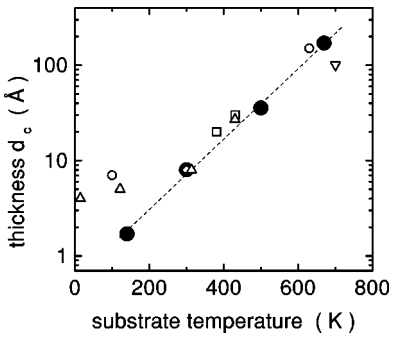

FIG. 7. Thickness for completion of substrate coverage at various substrate temperatures as derived from HAS (●). The size of the symbols is chosen to cover the error bars and the dotted line is a least-square-fit to the data. For comparison: thickness values for the onset of remanent magnetization (○, from Refs. 13,37), of dc conductivity (∇, from Ref. 30), and of Drude-like IR absorption (△, from Refs. 38,12); thicknesses close to the minimum values for local conductivity (□, from Ref. 11); the thickness where the dimensional crossover in the dc conductivity occurs (◇, from Ref. 13).

D. Complete coverage

For metal films the minimum thickness d_c (in units of the epitaxial monolayer thickness $h_{\mathrm{ML}} = 1.33$ Å), which is necessary for a complete coverage of the substrate surface with islands, is of particular relevance for an understanding of electronic,[13] magnetic,[13] IR optical,[12] and adsorbate spectroscopical[36] properties. A still open question is the correlation of percolation thresholds for structural and transport properties. Our HAS data allow an estimate of d_c over a wide range of temperatures. We consider that the ratio for the reduction of intensity due to complete coverage of the MgO substrate with Fe islands (as observed at 140 K) is 10^{-3} and that the intensity behavior is related to the lateral growth mode for the various temperatures. Solving Eqs. (6) and (7) for $d = d_c$ and setting $I(d_c)$ equal to the background scattering rate $I_{\min} = 10^{-3} I_{ns}$, we find

$$d_c = \gamma^{-1} \ln(I_{ns}/I_{\min}). \tag{10}$$

The results for the whole temperature range are shown in the logarithmic plot of Fig. 7, where the symbol size is chosen to cover the error bars. From a lot of other experiments (see Fig. 7) there is some evidence for the usefulness of our estimation as a lower limit for the onset of transport properties of continuous films. Magnetic measurements, e.g., find a minimum thickness of 7 and 150 Å for remanently magne-

tizable films grown at 100 K (Ref. 13) and at 630 K,[37] respectively. An onset of dc conductivity is found beween 693 and 743 K growth temperature for 10 nm thick films.[30] Films grown at ~300 K show a dimensional crossover in their dc conductivity at a thickness of 8 Å.[13] A STM study on Fe ultrathin-film growth on MgO was done on 20 and 30 Å thick films grown at 380 and 430 K, respectively[11] (the lack of local conductivity makes it impossible to do STM investigations on much thinner films). Very recent IR-spectroscopic measurements of Fe films grown on MgO(001) at temperatures from 14 to 430 K (Refs. 12,38) show a strong onset of Drude-like IR-absorption at the thicknesses indicated in Fig. 7.

For air-cleaved MgO, IR-absorption measurements[10] clearly reval a shift of d_c to lower values due to the higher defect density compared to UHV-cleaved substrates. At low substrate temperatures, the d_c values from HAS are smaller than those for the onset of bulklike transport from IR-optical conductivity or magnetic measurements. The differences are found for films of rather 2D islands with rough boundaries. Coalescence of such objects means the formation of defect rich regions. Both, the defect rich regions and the 2D character of the ordered regions should be origins of the observed differences. Above d_c, remanent magnetizability and dynamic conductivity starts as soon as the HAS intensity has regained a higher value (see plateau for 140 K).

VI. CONCLUSIONS AND SUMMARY

With HAS *in situ* measurements we investigated the growth of a metal on an insulating substrate. The measurements during metal deposition extended over well distinguishable growth phases: island nucleation, island growth, achievement of complete substrate coverage and island coalescence, island smoothing, and homoepitaxial growth. For deposition at various substrate temperatures, the island saturation density and the development of island size and island shape could be quantified.

For the island growth of Fe on UHV-cleaved MgO(001), we show that at a low temperature (140 K) weak substrate-island mass transport enables a fast substrate coverage but the surface is rough on atomic scale. At higher temperature almost 3D growth allows complete substrate coverage only at a higher film thickness by the coalescence of larger islands. The islands change their size and shape during growth. From a lateral growth parameter that corresponds to the observed experimental intensity decay we could determine the thickness for coalescence for a wide temperature range. The development of higher crystalline quality and smooth film surfaces is favored at higher temperatures, but the development of crystalline facets prevents the growth of a homogenous film. From these findings we propose a controlled growth procedure to gain ultrathin but smooth and homogenous films.[39] To reach fast substrate coverage, about 1 ML of Fe should be deposited at a low temperature (e.g., 140 K), whereas further growth should be at a temperature above room temperature to smooth out the granular morphology. In summary, the investigated system still appears as a good candidate (compared to other metal insulator combinations) for a conducting and magnetic ultrathin metal-on-insulator system. The variety of island shapes and high island densities might be advantageous for the investigation of shape specific catalytic and optical investigations.

ACKNOWLEDGMENTS

This work was part of the Sonderforschungsbereich 290. The authors would like to thank G. König for experimental assistance, G. Meyer, R. Koch, and K. Thürmer for many stimulating discussions, and the authors of Ref. 31 for sending a preprint prior to publication.

*Electronic address: fahsold@urz.uni-heidelberg.de
FAX: (49)6221-549262.

[1] Y. Park, E. Fullerton, and S. D. Bader, Appl. Phys. Lett. **66**, 2140 (1995).
[2] C. Li and A. J. Freeman, Phys. Rev. B **43**, 780 (1991).
[3] P. W. Palmberg, T. N. Rhodin, and C. J. Todd, Appl. Phys. Lett. **11**, 33 (1967).
[4] M. Meunier and C. R. Henry, Surf. Sci. **307**, 514 (1994).
[5] J. B. Zhou and T. Gustafsson, Surf. Sci. **375**, 221 (1997).
[6] T. Urano and T. Kanaji, J. Phys. Soc. Jpn. **57**, 3403 (1988).
[7] C. Duriez, C. Chapon, C. R. Henry, and J. M. Rickard, Surf. Sci. **230**, 123 (1990).
[8] T. Mühge, A. Stierle, N. Metoki, H. Zabel, and U. Pietsch, Appl. Phys. A: Solids Surf. **59**, 659 (1994).
[9] C. R. Henry and C. Chapon, J. Phys. (Paris) **46**, 1217 (1985).
[10] G. Fahsold, A. Priebe, N. Magg, and A. Pucci (Lehmann), Thin Solid Films (in press).
[11] J. F. Lawler, R. Schad, S. Jordan, and H. van Kempen, J. Magn. Magn. Mater. **165**, 224 (1997).
[12] G. Fahsold, A. Bartel, O. Krauth, and A. Lehmann, Surf. Sci. **433**, 162 (1999).
[13] C. Liu, Y. Park, and S. D. Bader, J. Magn. Magn. Mater. **111**, L225 (1992).
[14] L. Z. Mezey and J. Giber, Jpn. J. Appl. Phys., Part 1 **21**, 1569 (1982).
[15] S. H. Overbury, P. A. Bertrand, and G. A. Samorjai, Chem. Rev. **75**, 547 (1975).
[16] A. T. Yinnon, D. A. Lidar, R. B. Gerber, P. Zeppenfeld, M. A. Krzyzowski, and G. Comsa, Surf. Sci. **410**, L721 (1998).
[17] A. Lock, B. J. Hinch, and J. P. Toennies, in *Kinetics of Ordering and Growth at Surfaces*, edited by M. G. Lagally (Plenum, New York, 1990).
[18] G. Comsa and B. Poelsema, in *Atomic and Molecular Beam Methods*, edited by G. Scoles (Oxford University Press, Oxford, 1992), Vol. 2, p. 463.
[19] A. C. Levi and D. Paserone, Surf. Sci. **342**, 307 (1995).
[20] H. Brune, Surf. Sci. Rep. **31**, 121 (1998).
[21] G. König, Ph.D. thesis, Freie Universität Berlin, 1995.
[22] Crystal, Berlin, Germany.
[23] G. Fahsold (unpublished).
[24] J. P. Toennies and W. Kress, in *Surface Phonons*, Springer Series in Surface Science Vol. 21, edited by W. Kress and F. W. de Wette (Springer, Berlin, 1991), p. 111.
[25] K.-H. Rieder, Surf. Sci. **118**, 57 (1982).
[26] J. A. Stroscio, D. T. Pierce, and R. A. Dragoset, Phys. Rev. Lett. **70**, 3615 (1993).
[27] K. Thürmer, R. Koch, M. Weber, and K.-H. Rieder, Phys. Rev. Lett. **75**, 1767 (1995).

[28] G. Ehrlich and F. G. Hudda, J. Chem. Phys. **44**, 1039 (1966); R. L. Schwoebel, J. Appl. Phys. **40**, 614 (1969).
[29] B. M. Lairson, A. P. Payne, S. Brennan, N. M. Rensing, B. J. Daniels, and B. M. Clemens, J. Appl. Phys. **78**, 4449 (1995).
[30] S. M. Jordan, R. Schad, A. M. Keen, M. Bischoff, D. S. Schmool, and H. van Kempen, Phys. Rev. B **59**, 7350 (1999).
[31] G. Haas, A. Menck, H. Brune, J. V. Barth, J. A. Venables, and K. Kern, Phys. Rev. Lett. (to be published).
[32] V. Musolino, A. Selloni, and R. Car, Surf. Sci. **402-404**, 413 (1998).
[33] K. Sangwal, F. Sanz, J. Servat, and P. Gorostiza, Surf. Sci. **383**, 78 (1997).
[34] C. R. Henry and M. Meunier, Vacuum **50**, 157 (1998).
[35] R. Kunkel, B. Poelsma, L. K. Verheij, and G. Comsa, Phys. Rev. Lett. **65**, 733 (1990).
[36] O. Krauth, G. Fahsold, and A. Lehmann (Pucci), J. Chem. Phys. **110**, 3113 (1999).
[37] R. Koch (private communication).
[38] N. Magg, diploma thesis, Universität Heidelberg, 1999.
[39] A. Priebe, diploma thesis, Universität Heidelberg, 1999.